



**HAL**  
open science

# The role of seismicity models in probabilistic seismic hazard estimation: comparison of a zoning and a smoothing approach

C. Beauval, O. Scotti, F. Bonilla

► **To cite this version:**

C. Beauval, O. Scotti, F. Bonilla. The role of seismicity models in probabilistic seismic hazard estimation: comparison of a zoning and a smoothing approach. *Geophysical Journal International*, In press, 165 (2), pp.584-595. 10.1111/j.1365-246X.2006.02945.x . hal-00407583

**HAL Id: hal-00407583**

**<https://hal.science/hal-00407583v1>**

Submitted on 15 Oct 2021

**HAL** is a multi-disciplinary open access archive for the deposit and dissemination of scientific research documents, whether they are published or not. The documents may come from teaching and research institutions in France or abroad, or from public or private research centers.

L'archive ouverte pluridisciplinaire **HAL**, est destinée au dépôt et à la diffusion de documents scientifiques de niveau recherche, publiés ou non, émanant des établissements d'enseignement et de recherche français ou étrangers, des laboratoires publics ou privés.



Distributed under a Creative Commons Attribution 4.0 International License

# The role of seismicity models in probabilistic seismic hazard estimation: comparison of a zoning and a smoothing approach

Céline Beauval,<sup>1,2</sup> Oona Scotti<sup>1</sup> and Fabian Bonilla<sup>1</sup>

<sup>1</sup>IRSN/BERSSIN, BP 17, 92262 Fontenay-aux-Roses Cedex, France

<sup>2</sup>IRD - Géosciences Azur, 250 av. Albert Einstein, 06560 Valbonne, France. E-mail: beauval@geoazur.unice.fr

Accepted 2006 January 17. Received 2006 January 17; in original form 2005 September 5

## SUMMARY

Seismic hazard estimations are compared using two approaches based on two different seismicity models: one which models earthquake recurrence by applying the truncated Gutenberg-Richter law and a second one which smoothes the epicentre location of past events according to the fractal distribution of earthquakes in space (Woo 1996). The first method requires the definition of homogeneous source zones and the determination of maximum possible magnitudes whereas the second method requires the definition of a smoothing function. Our results show that the two approaches lead to similar hazard estimates in low seismicity regions. In regions of increased seismic activity, on the other hand, the smoothing approach yields systematically lower estimates than the zoning method. This epicentre-smoothing approach can thus be considered as a lower bound estimator for seismic hazard and can help in decision making in moderate seismicity regions where source zone definition and estimation of maximum possible magnitudes can lead to a wide variety of estimates due to lack of knowledge. The two approaches lead, however, to very different earthquake scenarios. Disaggregation studies at a representative number of sites show that if the distributions of contributions according to source–site distance are comparable between the two approaches, the distributions of contributions according to magnitude differ, reflecting the very different seismicity models used. The epicentre-smoothing method leads to scenarios with predominantly intermediate magnitudes events ( $5 \leq M \leq 5.5$ ) while the zoning method leads to scenarios with magnitudes that increase with the return period from the minimum to the maximum magnitudes considered. These trends demonstrate that the seismicity model used plays a fundamental role in the determination of the controlling scenarios and ways to discriminate between the most appropriate models remains an important issue.

**Key words:** low-seismicity regions, probabilistic methods, seismic hazard assessment, seismic modelling, seismicity, sensitivity.

## 1 INTRODUCTION

In every region of the world where significant earthquakes may occur, seismic hazard has to be evaluated in order to produce hazard maps used for mitigation purposes. In regions where the instrumental seismicity is low to moderate and strong earthquakes have nonetheless occurred in the past, the estimation of hazard has to cope with the small amount of data available. Such regions are for example the Eastern parts of the United States or the northern regions of Europe. In this paper we study France as an example of such moderate seismicity regions. A few strong earthquakes have occurred in the past, with magnitudes between 6.0 and 7.0 (e.g. the Lambesc earthquake at the beginning of the 19th century (Baroux *et al.* 2003), or the Bâle earthquake in the 14th century, ECOS catalogue of Switzerland, <http://histserver.ethz.ch>). The country has been covered by an instrumental seismological network since the

early 1960s (Nicolas *et al.* 1998) and large efforts have enabled to gather historical information on earthquake occurrences in the last 700 yr (Levret *et al.* 1994).

The seismic hazard for France has been estimated using probabilistic methods only recently (Dominique *et al.* 1998; Martin *et al.* 2002b; Beauval & Scotti 2004; Marin *et al.* 2004). The classical method used for the computation of probabilistic seismic hazard, in France and worldwide, is a zoning method and was initiated by Cornell (1968) and McGuire (McGuire 1976). This zoning approach requires the modelling of the recurrence of earthquakes in each seismic source zone, that is, the computation of the Gutenberg-Richter parameters (Gutenberg & Richter 1944; Kramer 1996). The major problem with the definition of seismic sources is that unfortunately, except in highly active regions where well-characterized faulting dominates, there is usually no clear understanding of the processes that give rise to earthquakes and large geographical areas are

delineated. Different experts often provide very different maps that characterize somewhat different zonation schemes, based on their differing interpretations of the meagre data that exist. The definition of homogeneous source zones, which are based on a combination of different seismotectonic criteria, are often highly questioned in the scientific community, mainly because the seismicity is assumed homogeneous inside each source zone and because obviously the limits of the source zones control the distribution of hazard estimates. Moreover, in low seismicity regions where seismic data are scarce, the computation of the recurrence curve parameters is difficult and questionable (see e.g. Beauval & Scotti 2003) and the determination of the maximum magnitude used for truncating the recurrence curve is the subject of great discussions. Different methodologies have been proposed in the literature to face these problems. Bender & Perkins (1993) have proposed a smoothing of the hazard estimates at the border between two source zones. This is convenient and prevents high gradients values between two neighbouring geographical sites but there is no scientific justification in this smoothing. Another way of handling the uncertainty on the delineation of seismic sources is the use of logic trees: several zonings are considered and the final hazard corresponds to a mean (or median) value. Moreover, a modified version of the zoning method was proposed by Frankel (1995) for the probabilistic seismic hazard of the Eastern U.S.: the region of interest is covered by a grid, the source zones are simply the square cells and the cumulative number of events are counted inside each cell. Then the cumulated seismic rate grid is smoothed

with a Gaussian function and finally a regional  $b$ -value is attributed to consider a Gutenberg-Richter recurrence inside each cell. These variants of the zoning method are not studied here.

We propose in this study to analyse the smoothing method proposed by Woo (1996) relying on the fractal distribution of earthquakes in space. The difference between the zoning approach and Woo's smoothing method lies in the seismicity model; whereas the zoning method requires homogeneous source zones and a frequency-magnitude distribution for each source zone, Woo (Woo 1996) proposes to use maps of smoothed epicentre locations. The epicentre location of events is smoothed according to the fractal distribution of earthquakes in space (e.g. Kagan & Jackson 2000). The total annual seismic rate over the region is thus the same as the rate computed from the seismic catalogue, but the annual rate densities are distributed over the region. By not requiring the delineation of source zones and the modelling of earthquake recurrence, Woo's method can be considered as an alternative method to bypass these difficulties. On the other hand, this epicentre-smoothing method brings its own uncertainties, such as the choice of the smoothing function. Also, it does not allow for the occurrence of magnitudes greater than the maximum magnitude observed, unless the uncertainties on magnitude determinations or some background seismicity are added (Woo 1996). The advantages and disadvantages of each method and the consequences on hazard estimation are compared in this study, at the scale of the French territory, through hazard levels and controlling seismic scenarios. Note that the aim of the present

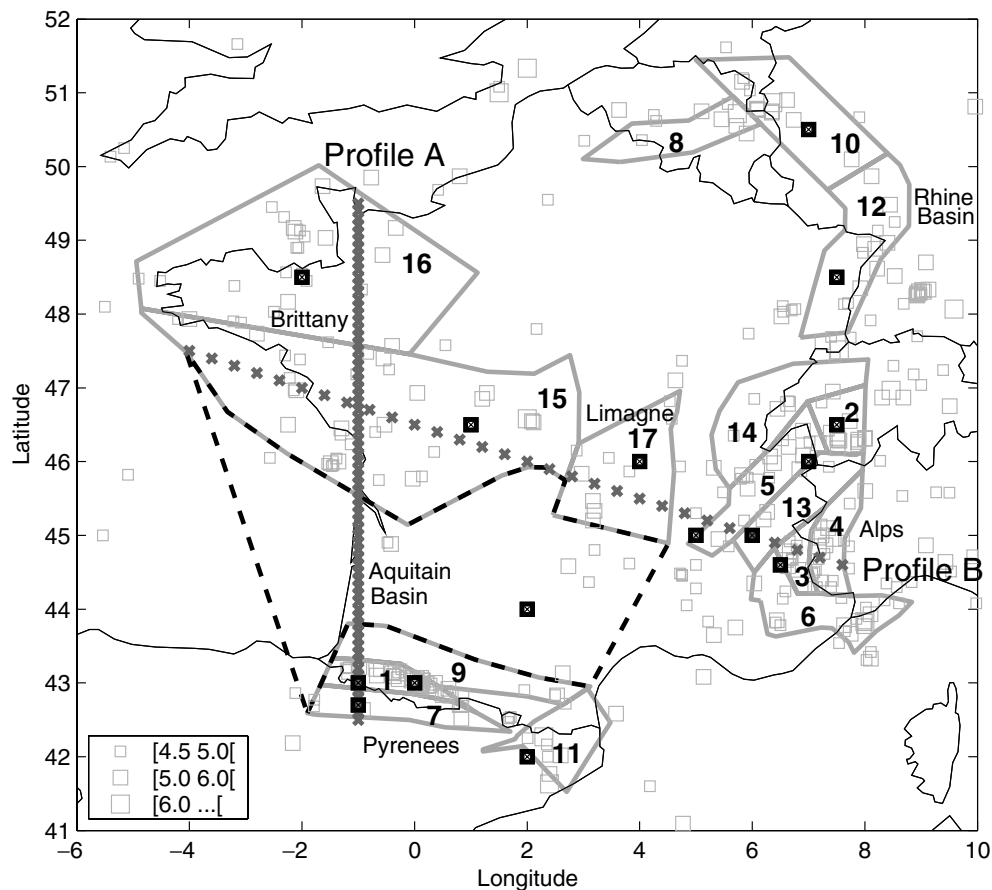


**Figure 1.** Seismicity, source zones limits and geographical sites considered in this study. Grey squares: seismic events  $M \geq 4.5$  in the French catalogue [1356–1999]. Grey solid lines: the 17 source zones used in the zoning approach, selected from the zoning proposed by Autran *et al.* (1998) (numbers are indicated). Grey crosses: profiles A and B (see Section 3). Dashed lines: limits of the background source zone used (see Section 3.3). Dark squares: sites used for the study on seismic scenarios (see Section 4).

**Table 1.** Completeness periods used for the computation of the recurrence parameters on magnitudes equal or above 3.5.

Interval	[3.5–4.4]	[4.5–4.9]	[5.0–5.4]	[5.5–5.9]	[6.0–6.4]	[6.5–...]
Time period	[1962–1999]	[1900–1999]	[1870–1999]	[1800–1999]	[1300–1999]	[1300–1999]

study is not to give a comprehensive range of possible hazard values for the regions under study. The smoothing approach proposed by Woo is tested and compared to the classical zoning method in order to determine if it could be applied in very low seismicity regions where the delineation of seismic sources and modelling of recurrence is highly questionable.

## 2 PROBABILISTIC HAZARD ESTIMATION

### 2.1 Seismic data

The seismic catalogue used in this study is composed of an instrumental part 1962–1999 and an historical part 1356–1961 (Fig. 1). The instrumental catalogue of the Laboratoire de Détection et de Géophysique (LDG, Commissariat à l’Energie Atomique, Bruyères le Châtel) reporting homogeneous local magnitude  $M_L$  is used (Nicolas *et al.* 1998). The geographical window  $[-5^\circ \text{ } 9^\circ]$  in longitude and  $[42^\circ \text{ } 51^\circ]$  in latitude is considered. The intensities of the historical database SisFrance are converted into magnitudes using the Levret correlation (Levret *et al.* 1994). The corresponding completeness periods have been estimated and are reported in Table 1.

### 2.2 Probabilistic computation

The minimum magnitude for the PSHA computation is fixed to 4.5. The Berge-Thierry *et al.* (2003) attenuation relationship is used here. To compute probabilities of exceedance of ground motions, the Gaussian probability distribution predicted by the attenuation relationship is truncated at two standard deviations above the mean. Such a truncation is performed in order to prevent accelerations with extremely low probabilities of occurrence to contribute extensively to the hazard (see e.g. Beauval & Scotti 2004). For simplicity in the computations, all depths of source zones are fixed to 10 km in the zoning seismicity model (mean depth of earthquakes in France, Autran *et al.* 1998), and all earthquakes are attributed a 10 km depth in the smoothing seismicity model.

#### 2.2.1 Zoning method

In our computation of hazard based on the zoning method, we work with the Fortran code CRISIS by M. Ordaz modified mainly to handle different types of attenuation relationships through analytical formulations rather than tables (original version <http://www.ifjf.uib.no/seismo/software/seisan/seisan.html>). The main characteristic of this code is the discretization of source zones: they are subdivided into unit triangular areas, with triangle dimension increasing as the triangle moves away from the site. The zoning used here is based on the area limits proposed by Autran *et al.* 1998, also used for the establishment of the new seismic zonation for France (Martin *et al.* 2002a). From the initial zoning covering France and its frontiers, 17 source zones have been selected (see Beauval 2003; Beauval & Scotti 2004). The selection ensures a minimum number of events inside the source zone and the reliability of the recurrence parameters (Table 2). The probabilistic hazard estimation inside these 17 source zones is not affected by the very low seismicity located outside these source zones. The observed maxi-

**Table 2.** Seismic parameters for the 17 source zones, determined with Weichert’s method (Weichert 1980) (annual seismic rate for  $M \geq 4.5$ :  $\lambda$ , and slope of the Gutenberg-Richter curve  $\beta$ ). Maximum magnitudes in the time period [1356–1999] computed with the Levret correlation (Levret *et al.* 1994).  $\lambda_{\text{norm}}$  is normalized to a  $100 \times 100 \text{ km}^2$  area, source zones are listed in decreasing  $\lambda_{\text{norm}}$  order.

Zone	$\lambda(M \geq 4.5)$	$\beta$	$M_{\text{Max}}^{\text{Obs}}$	$\lambda_{\text{norm}}$
1	0.2724	2.69	6.0	0.4064
2	0.1455	1.78	5.9	0.2502
3	0.0680	1.99	5.5	0.1757
4	0.1351	2.12	5.5	0.1719
5	0.1491	2.13	5.6	0.1180
6	0.1154	2.44	6.2	0.0817
7	0.0517	2.59	5.7	0.0505
8	0.0462	2.33	6.0	0.0479
9	0.0569	3.27	5.6	0.0359
10	0.0684	2.39	6.1	0.0333
11	0.0321	2.53	6.0	0.0288
12	0.0541	1.83	5.9	0.0274
13	0.0355	2.56	5.6	0.0267
14	0.0416	2.39	5.4	0.0231
15	0.2105	2.68	6.1	0.0216
16	0.1206	2.19	5.5	0.0161
17	0.0251	2.25	5.7	0.0103

imum magnitudes of source zones and the seismicity parameters are reported in Table 2. In order to test the influence on hazard of the uncertainty on maximum magnitude, two hazard computations are performed: one uses the maximum observed historical magnitudes, and the other uses the same magnitudes increased by 0.5 magnitude degree (mean uncertainty on historical magnitude, Beauval 2003).

#### 2.2.2 Epicentre-smoothing method

In the smoothing method proposed by Woo (1996), maps of past epicentres are spatially smoothed in order to obtain maps of annual seismic rates for all magnitudes. We work with the codes written by G. Woo. The seismic rate maps are computed with  $5 \times 5 \text{ km}$  square unit areas. The kernel function used to smooth epicentres relies on Vere-Jones (1992)’s statistical analyses of catalogues, in order to reproduce the fractal distribution of earthquakes in space:

$$K(r) = \frac{\lambda - 1}{\pi} \frac{1}{r_s^2} \left( 1 + \frac{r^2}{r_s^2} \right)^{-\lambda} \quad \lambda \in [1.5-2.0], \quad (1)$$

with  $\lambda$  controlling the degree of spatial smoothing. In the following, both values 1.5 and 2.0 will be used in the hazard computations, showing that the choice of this parameter has a negligible influence on hazard estimates. Following Woo (1996) and Molina *et al.* (2001), we used the function  $r_s$ :

$$r_s(m) = H e^{km}, \quad (2)$$

with  $H = 0.26$  and  $k = 0.96$ . The parameters  $H$  and  $k$  controlling the shape of the kernel were calibrated on the French catalogue using the methodology proposed by Molina *et al.* (2001). Events are binned into 0.5-large magnitude intervals. Within each magnitude interval, the distance  $r$  to the nearest event is computed for each

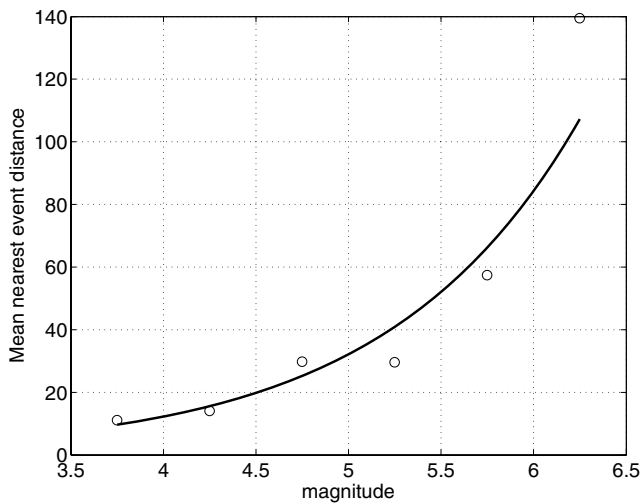


**Figure 2.** Bandwidth function  $r_s(m) = He^{km}$ , computed from the whole seismic catalogue covering the time period 1356–1999, in the window  $[-5^\circ 9^\circ] \times [42^\circ 51^\circ]$  (cf. text).

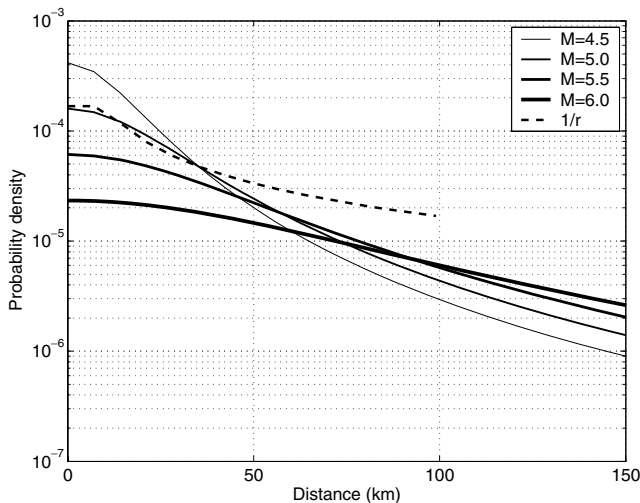


**Figure 3.** Spatial kernel functions (displayed in 1 dimension) used to smooth epicentres maps. Solid line: Vere-Jones kernel, the higher the magnitude, the stronger the smoothing. Dashed line:  $1/r$  truncated kernel, with maximum distance 100 km.

event, the mean of all distances is then computed (mean nearest event distance). A regression is performed on these mean distances to compute parameters  $H$  and  $k$  (see Fig. 2). The kernel functions used to smooth magnitudes 4.5–6.0 are displayed on Fig. 3. The lower the magnitude is, the weaker the spatial smoothing is, reflecting the increase of clustering. A grid of seismic rates is computed for each magnitude above the minimum magnitude with 0.1-magnitude increment. As an example, the grid (or annual rates map) is displayed here for the magnitude degree 5.3 (Fig. 4). This grid is used for the computation of hazard at the site (6.6°; 44.6°) located in the Alps. The original epicentres of magnitude 5.3 are also displayed. The occurrence of each event is thus distributed over the whole space, the probability of occurrence decreases with the distance between the cell and the original location of the event.

Note that Woo’s method permits easily to take into account uncertainties on magnitude determination, by using probability density functions (Woo 1996). Doing this would enable to take into account

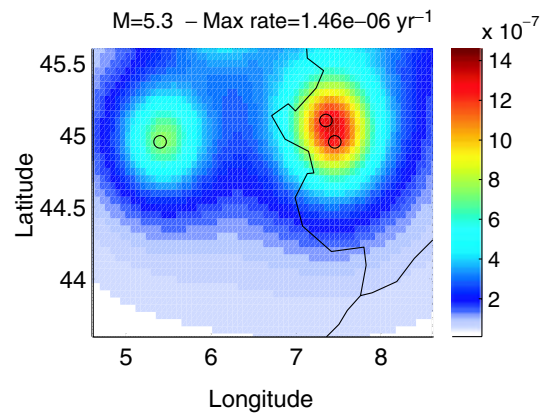


**Figure 4.** Example of an annual seismicity rate map for magnitude degree 5.3 (smoothing approach). Grid of cells 5 km  $\times$  5 km used to compute the hazard at the site with longitude 6.6° and latitude 44.6°. Circles: smoothed observed epicentres.

larger magnitudes than the historical ones. However, as estimating the uncertainties on historical magnitude determination is rather difficult and subjective, this option is not included here in order to use only the information brought by the spatial smoothing of historical epicentres. Our aim is not to give a comprehensive range of possible hazard values for the studied region, but to compare two probabilistic methodologies.

### 3 COMPARISONS OF HAZARD LEVELS BASED ON THE ZONING AND EPICENTRE-SMOOTHING METHODS

In order to be able to compare acceleration levels, hazard is computed along two profiles, crossing low and moderate seismicity regions. Hazard is estimated for three return periods: 475,  $10^4$  and  $10^5$  yr. Through a profile comparison, we aim to relate the differences between smoothing and zoning hazard levels directly to the seismic activity of each region.

#### 3.1 Results on two profiles

The first profile (A) is along the meridian  $-1$  (see Figs 1 and 5), thus crossing first the West Pyrenees then the Aquitaine Basin and finally Brittany. For the three return periods, hazard estimates in the two source zones of Brittany are comparable for both methods, with the smoothing hazard estimates following closely the seismicity density and the zoning estimates being uniform over each source zone. On the contrary, hazard estimations differ significantly for the sites located inside source zone 1: estimates based on zoning are much higher than estimates based on the smoothing method with acceleration values reaching up to 0.21 g for the former and only up to 0.13 g for the latter at 475 yr return period. This narrow Pyrenees zone has the highest seismic rate among the 17 source zones considered (cf. Table 2). In this case, the zoning method concentrates the seismicity in a narrow region leading to a higher hazard. In the Brittany region, on the other hand, the zoning approach distributes the seismicity over a very wide region and the smoothing method can provide locally higher hazard levels than the zoning method at short return periods (475 yr). For longer return periods, the estimates based on the smoothing approach are either equal or lower than the estimates based on the zoning approach. The estimates obtained outside the source zones (in the Aquitaine Basin, latitudes

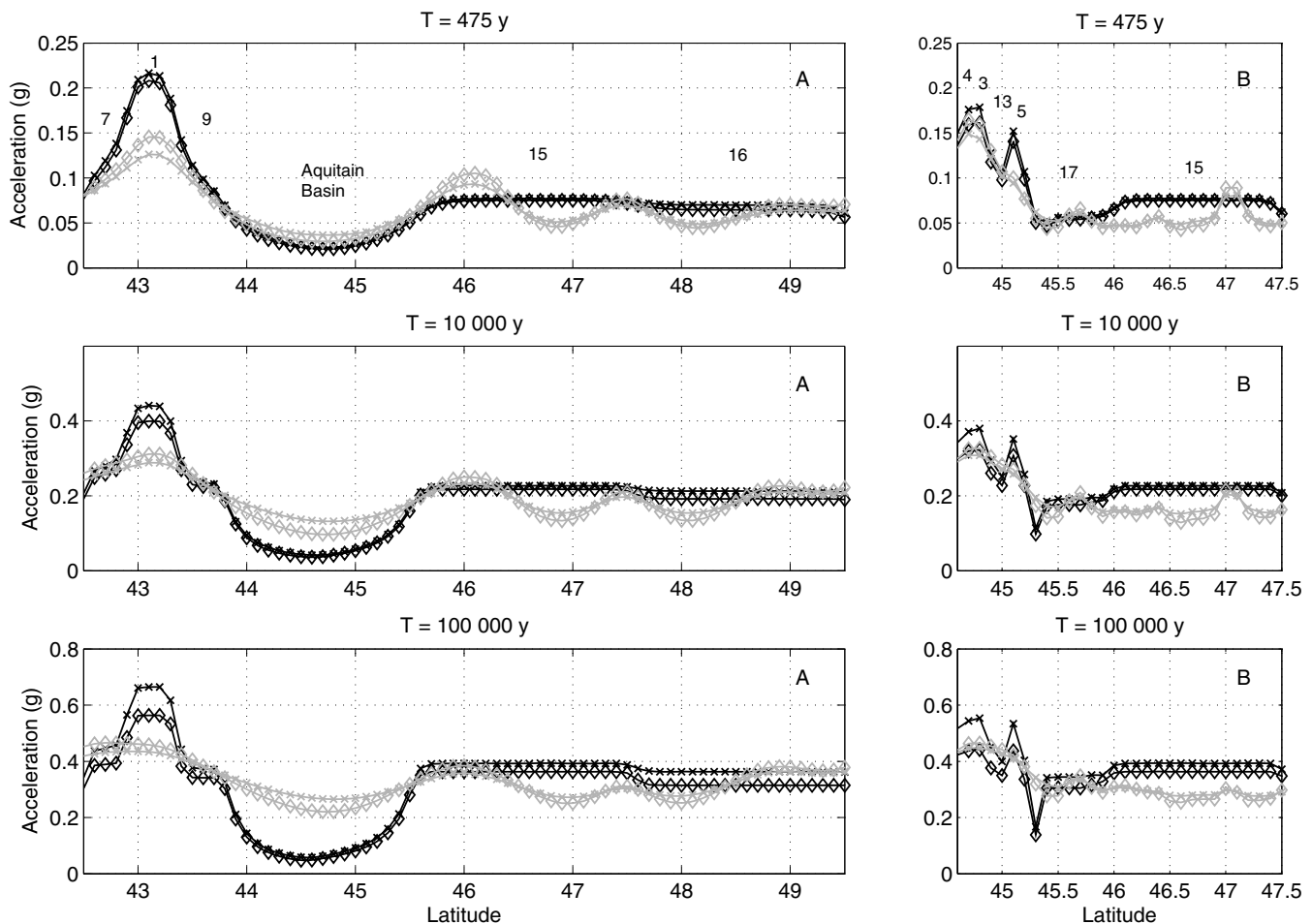


**Figure 5.** PGA hazard levels along the 2 profiles considered in this study (Fig. 1) for return periods 475,  $10^4$  and  $10^5$  yr. Grey: estimates based on the smoothing method (crosses corresponds to  $\lambda = 1.5$ , diamonds to  $\lambda = 2.0$ ); dark: estimates based on the zoning method (crosses corresponds to  $M_{\max} = M_{\max}^{\text{obs}} + 0.5$ , diamonds to  $M_{\max} = M_{\max}^{\text{obs}}$ ). Numbers of source zones are indicated.

between  $44^\circ$  and  $44.5^\circ$ ) will be addressed later. The second profile is transversal (Profile B, Figs 1 and 5), crossing first the Alps, then the low seismicity Limagne zone, and finally Brittany. Similar trends are observed in the Alps and in Limagne: in source zones with high seismic rates (zones 3, 4 and 5), the zoning method yields higher hazard values than the smoothing method (15–30 per cent increase); whereas smoothing results are similar to results based on the zoning method inside source zones with low to moderate seismic rate (source zones 13 and 17). However, in Brittany, the smoothing levels are systematically lower than the zoning ones, compared to profile A, this difference is due to a 3-D effect in the smoothing approach for these sites.

### 3.2 Influence of $M_{\max}$ and of smoothing function

The results also show that varying the maximum magnitude (zoning approach) or the kernel smoothing function (smoothing approach) does not influence much the hazard estimates. A 0.5 magnitude degree difference in the maximum magnitude attributed to the source zone (Fig. 5) only begins to produce a significant difference in the zoning estimation for very long return periods and in high seismicity zones (Pyrenees zone 1 or Alps zone 4).

Following Woo (1996) and Molina *et al.* (2001), the Vere-Jones kernel function has been used to smooth past earthquake locations.

A test shows that the choice of the  $\lambda$  parameter (eq. 1) has a negligible influence on hazard (Fig. 5). Moreover, several functions could be used such as simple kernels  $1/r$  and Gaussian functions (e.g. Kagan & Jackson 1994 or Cao *et al.* 1996). In order to evaluate the impact of the choice of the kernel on the hazard results, accelerations are computed with a  $1/r$  function truncated at 100 km (Fig. 3). In this case, the smoothing function no longer depends on the magnitude. The results are rather unexpected (Fig. 6): inside the source zones, hazard values remain stable along both profiles. Thus, in moderate and low seismicity regions, the choice of the kernel (both its shape and finite aspect) has a negligible impact on hazard. However, outside the seismotectonic source zones, in very low seismicity zones, and for return periods  $10^4$  and  $10^5$  yr, the impact is important: hazard estimates go down to very low values (0.05 g) in the Aquitaine Basin, similar to the zoning estimates when no background source zone is included. Therefore, while the shape of the kernel proves not to influence hazard estimations, the finite aspect of the kernel has a great impact on hazard estimates at large return periods in very low seismicity regions, yielding potentially underestimated hazard values. Note that the choice of the maximum distance was made following the work of Martin *et al.* (2002a). The truncation distance value remains arbitrary and if this finite function  $1/r$  is used in PSHA studies with very low probabilities, further work is needed to determine this upper bound distance.

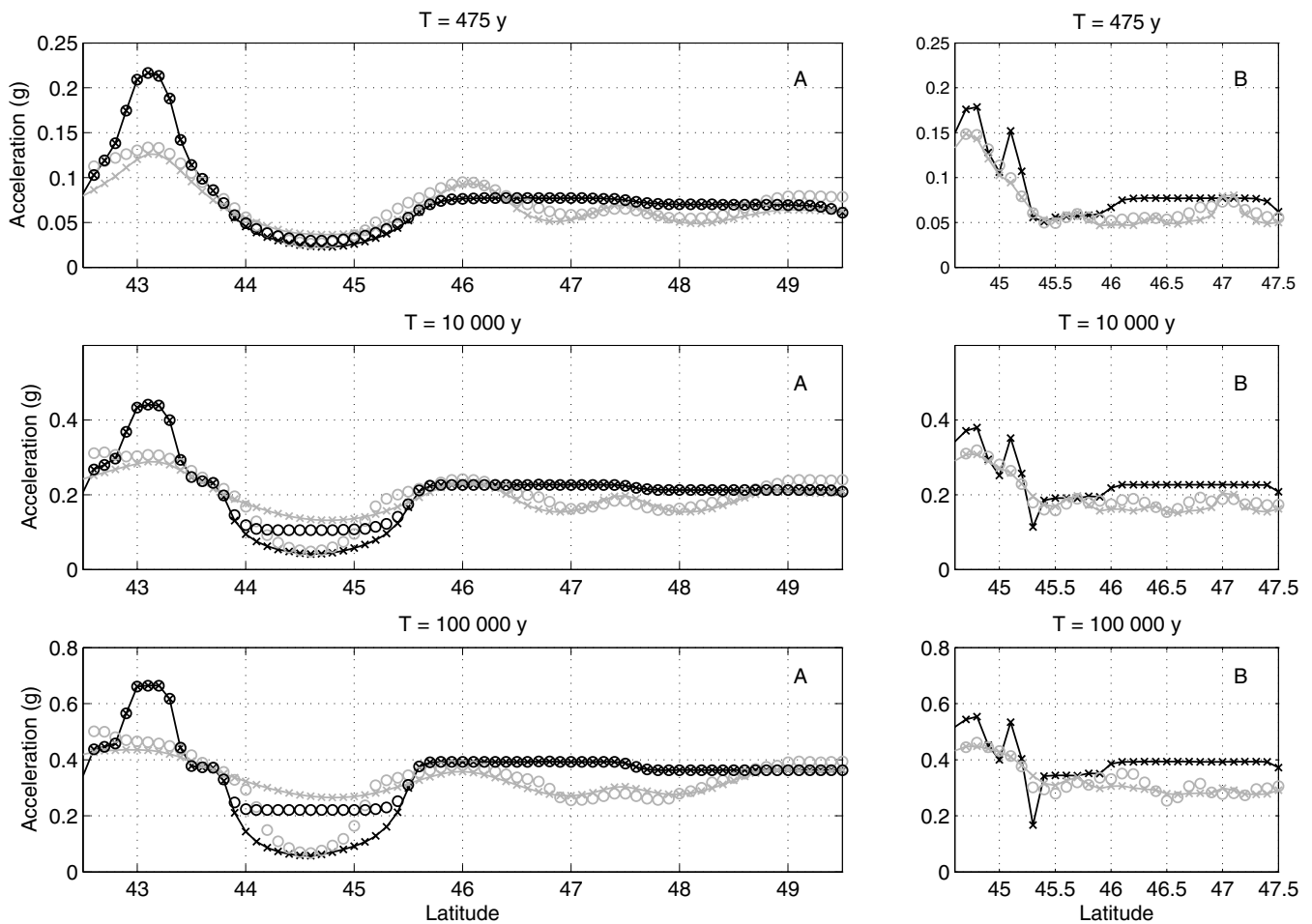


**Figure 6.** Influence of the choice of the smoothing function and estimation of hazard in very low seismicity regions. Grey: estimates based on the smoothing method (crosses when using magnitude-dependent kernels, circles when using a finite  $1/r$  function); dark: estimates based on the zoning method (crosses for estimation with source zones of Fig. 1, circles for estimation with a background source zone added to the seismicity model in the Aquitaine Basin, see Fig. 1).

### 3.3 PSHA in very low seismicity regions

Between latitudes  $44^\circ$  and  $45.5^\circ$ , the profile A crosses the Aquitaine Basin, a large area where very few seismic events occurred in the past and where it is very difficult to establish reliable earthquake recurrence models. Up to now, this region was not considered as an active source in the zoning approach. This accounts for the increasing difference between the two approaches with increased return period. In the following exercise, we delineate and activate a background source zone including the Aquitaine Basin (Fig. 1). We calculate the seismicity parameters in spite of the uncertainty involved and attribute the smaller maximum magnitude of all 17 zones (i.e. M5.4). With the addition of this background seismicity zone in the seismicity model of the zoning approach, the two methodologies produce very similar hazard levels (Fig. 6).

### 3.4 Conclusions on the hazard levels

Based on these results in France, we conclude that Woo's smoothing method can be considered as a lower bound estimator in comparison with the zoning method. This study is coherent with the conclusions of Molina *et al.* (2001), and generalizes their results based on the estimation of hazard at three sites in Southern Spain and in Norway. Moreover, we show that the smoothing results do not depend

strongly on the shape of the smoothing function used, an important result given the uncertainty on the determination of this function. Hazard results obtained at other frequencies (1, 2 and 5 Hz) lead to similar conclusions. Most importantly, the epicentre-smoothing method may provide the means to map minimum hazard levels in low seismicity regions where the establishment of recurrence curves remains extremely difficult.

## 4 CONTRIBUTING SEISMIC SCENARIOS

For a specific return period, we discussed the estimation of the corresponding hazard value. Although many hazard studies only require maps, it is also important to compare the deterministic scenarios that each methodology may lead to. Disaggregation results (Chapman 1995; Bazzurro & Cornell 1999) are often needed in PSHA studies to determine the contributing seismic scenarios. For site-specific probabilistic seismic hazard studies, the controlling seismic scenario is of utmost importance since it is used to characterize the seismic hazard at the site. Previous studies proposed to deduce scenarios from a large range of procedures: accumulating contributions to hazard in 1-D M bins, in 2-D M-R bins and in 3-D M-R- $\epsilon$  bins ( $\epsilon$  measures the deviation of the ground motion from the predicted median value, see Bazzurro & Cornell 1999, for a review of the

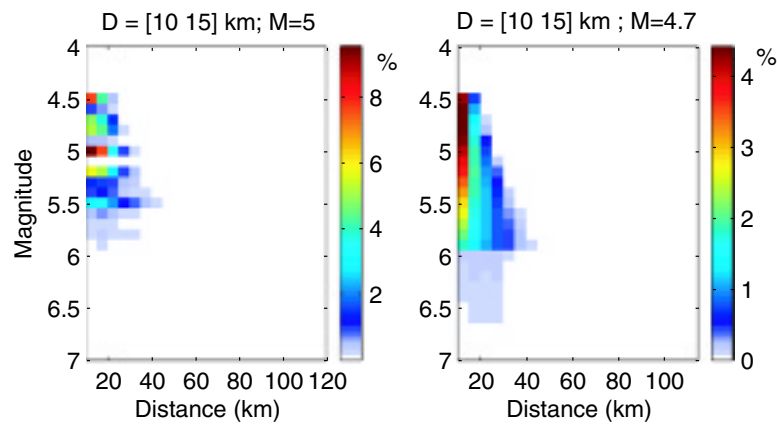


**Figure 7.** Disaggregation in 2-D, according to magnitude and distance, at the site ( $6.6^\circ; 44.6^\circ$ ) and for the return period 475 yr. On the left: smoothing disaggregation, corresponding to the acceleration  $A = 0.135$  g. On the right: zoning disaggregation,  $A = 0.168$  g. The magnitude-distance couple contributing the most to the hazard is indicated in the title.

procedures). Some studies propose to deduce these mean or mode seismic scenarios even when the disaggregation results are rather diffuse (e.g. Halchuck & Adams 2004; Choi *et al.* 2003). As there is no consensus on the way of deriving seismic scenarios, we decided to select the couple M-R producing the highest contribution to the hazard, which is in mathematical terms the bivariate modal values. Thus the seismic scenario corresponds to the most likely scenario and necessarily refers to an actual realizable source within the resolution of the magnitude and distance binning (contrary to means).

#### 4.1 Example site in the Alps

Fig. 7 displays the disaggregation results in 2-D, that is, the distribution of contributions to the hazard according to the magnitude and the distance, for the site ( $6.6^\circ; 44.6^\circ$ ) at 475 yr return period ( $A_{\text{zoning}} = 0.135$  g and  $A_{\text{smoothing}} = 0.168$  g). Contributions are normalized by the total hazard and expressed in percentage. The resulting seismic scenario is  $M = 5.0$  at  $R = 10\text{--}15$  km for the smoothing approach and  $M = 4.7$  at a hypocentral distance  $R = 10\text{--}15$  km for the zoning approach. As the 2-D distribution is obtained by binning distances in 5-km-large intervals, the scenario is characterized by an interval of distances, rather than by a unique distance. The depth of the events and source zones have been fixed to 10 km, thus the earthquake scenario may occur inside a disc centred at the site. Note that the determination of the most contributing distance is highly dependent on the binning used; thus, for the scenario study to be complete, different distance binnings should be considered. The scenario can be simply retrieved from the 2-D distributions, because spatial disaggregations (Fig. 8) show that, for both methods, the distribution of contributions in space is roughly isotropic with a maximum located at the site. Incidentally, the distribution of contributions shows that, for the smoothing method, the small rates of occurrence located near the site produce higher contributions to the hazard than the high rates located far from the site (near the epicentre locations). This result demonstrates the key role of the distance parameter in the attenuation relationship.

Disaggregation results are also displayed in 1-D on Fig. 9: all contributions are distributed according to one parameter, distance or magnitude. Note that for both methods, the magnitude of the scenario selected in 2-D does not correspond exactly to the magnitude with the maximum contribution in 1-D (bivariate and uni-

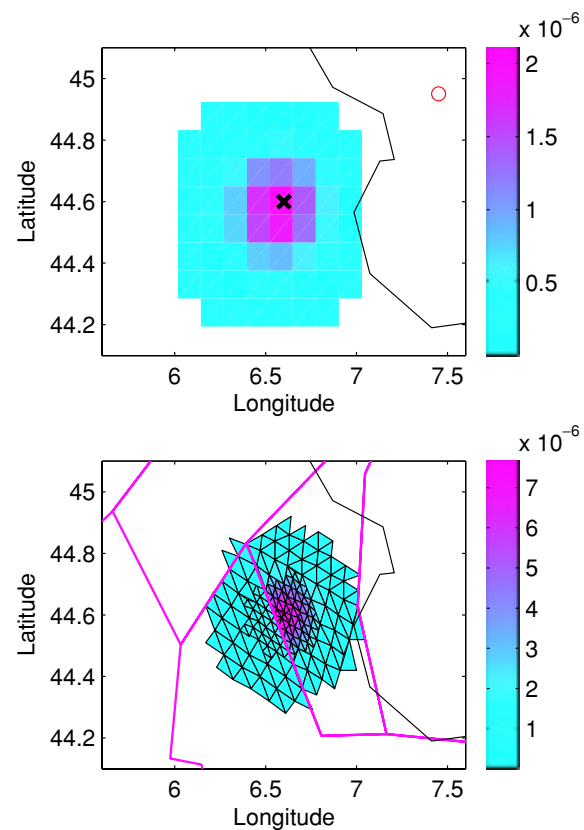


**Figure 8.** Example of spatial disaggregation, corresponding to the magnitude degree 5.3 at the site ( $6.6^\circ; 44.6^\circ$ ) and for the return period 475 yr (PGA). The colour bar indicates the contribution of each unit used in the computation (annual exceedance rate). Unit areas are squared cells in the smoothing method ( $5 \times 5$  km), and triangles in the zoning one (due to the way of discretizing source zones in CRISIS's computer code).

variate modes are not necessarily coincident, Bazzurro & Cornell 1999). The distributions of contributions according to the distance are rather similar between both methods: the smaller the distance between the source and the site, the higher the contribution to the hazard. On the contrary, the distribution of contributions according to the magnitude differ significantly. In the smoothing approach, the magnitude distribution presents peaks reflecting the history of



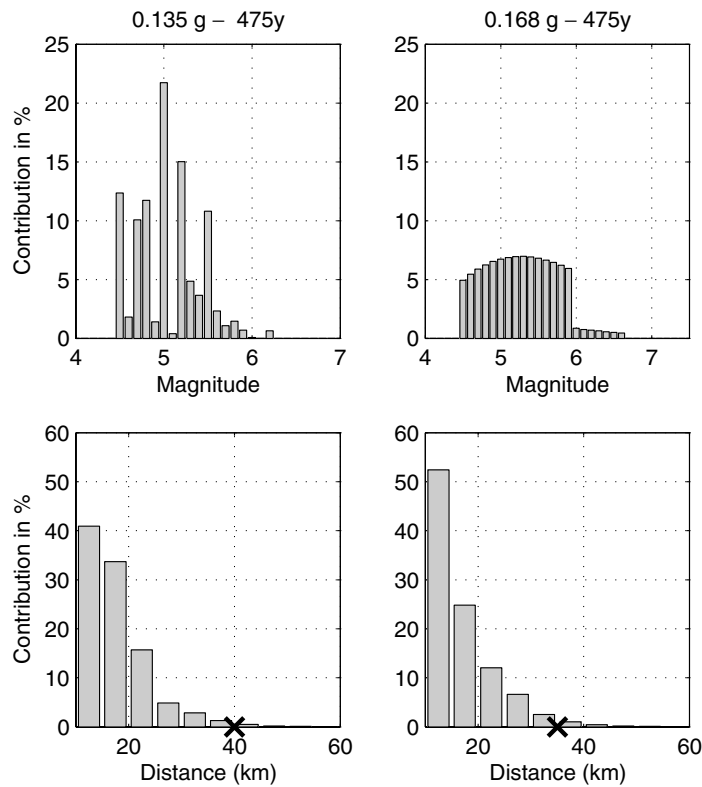


**Figure 9.** Disaggregation in 1-D for the studied site (6.6°;44.6°) at the return period 475 yr. Left: smoothing method; right: zoning. Upper panels: distributions of contribution to hazard according to the magnitude. Lower panels: distributions according to the distance (distances binned into 5 km-large intervals). Crosses correspond to the distance reached when 98 per cent of the contributions to the hazard are accumulated.

actual magnitudes observed in the past in the vicinity of the site. In the zoning approach, the distribution is smooth due to the use of the Gutenberg-Richter curve, with all magnitudes between the minimum and the maximum participating to the hazard. As large source zones have to be used in such moderate seismicity region, the contributions to the hazard come mainly from one source zone: the zone where the site is located.

An advantage of the smoothing approach is that the scenario can be directly attributed to the earthquake(s), or the epicentre(s), that is(are) contributing the most to the hazard, thus providing a direct link with the purely deterministic approach. An example of this epicentral disaggregation is displayed on Fig. 10. The geographical location of the seismic event contributing the most, a 4.5 magnitude earthquake, is thus identified. Note that magnitudes 5–5.2 in the vicinity of the site are also contributing to the hazard at this site.

#### 4.2 Example site in the Rhine Basin

The second site studied (7.5°;48.5°) is located in the Rhine Basin (source zone 12, Fig. 1). The hazard levels based on both probabilistic methods are comparable (0.085 g and 0.093 g) but disaggregation results differ significantly in magnitude. Results are first displayed for a return period of 475 yr (Fig. 11). The magnitude of the scenario is 4.9 for the smoothing method and 4.5 for the zoning one.

The scenarios deduced for the 10<sup>4</sup> yr return period (Fig. 12), yield greater magnitudes in both approaches: 5.4 for the smoothing approach and 5.6 for the zoning one. The acceleration levels are still comparable (0.24 g smoothing and 0.28 g zoning). In the zoning approach, the peak of 1-D contributions in magnitudes has shifted to the maximum magnitude attributed to source zone 12

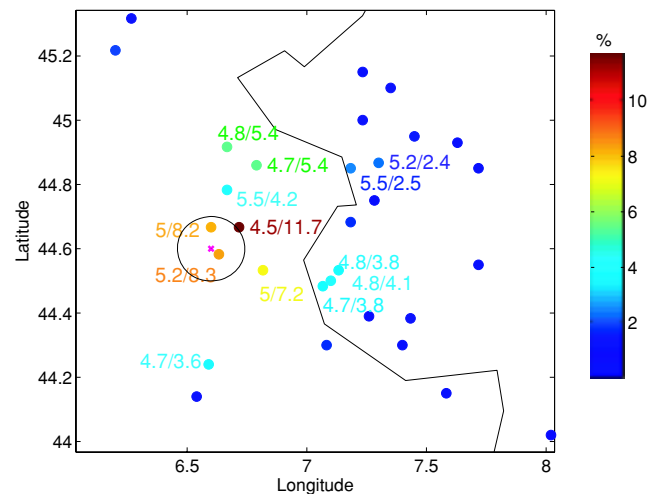


**Figure 10.** Epicentral disaggregation of hazard estimate based on the smoothing method for return period 475 yr and at the site (6.6°;44.6°). The colour attributed to each earthquake corresponds to its contribution to the hazard (expressed in percentage). Magnitudes and contributions greater than 2 per cent are indicated. For this example, the 4.5 magnitude event located northeast of the site is bringing the higher contribution. The black circle gives the limits of the possible location of the seismic scenario deduced from 2-D disaggregation.

(0.5 magnitude degree added to historical maximum magnitude). On the contrary, the distribution for 1-D contributions based on the smoothing approach has remained quite stable, changes occur only for magnitudes lower than 5.0 with a much lower participation to

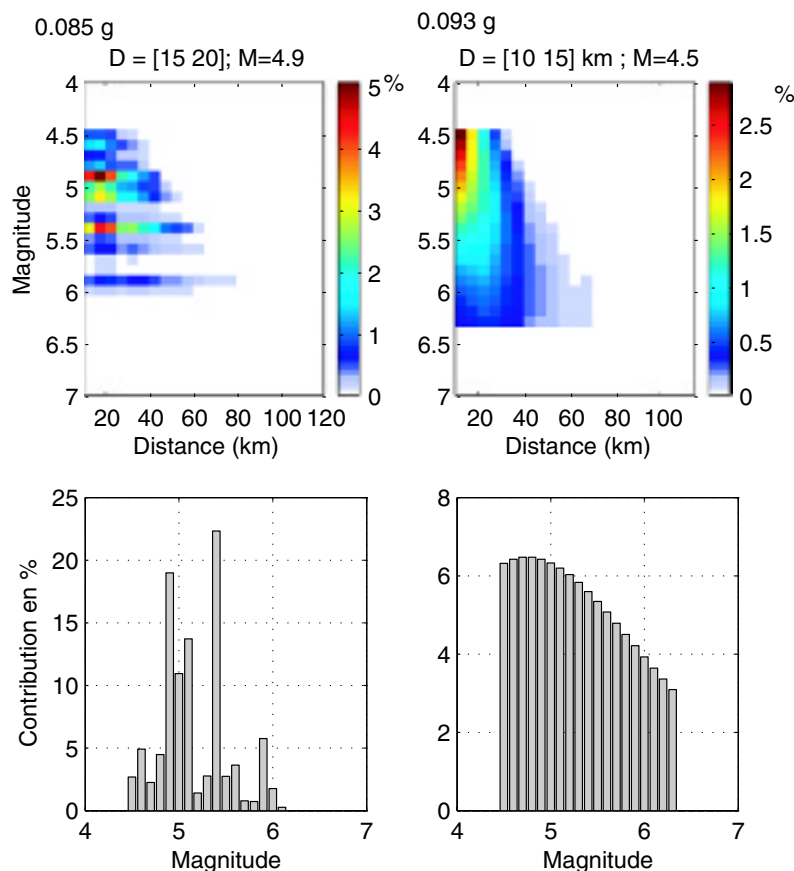


**Figure 11.** 2-D and 1-D disaggregations at the site with longitude  $7.5^\circ$  and latitude  $48.5^\circ$  located in the Rhine Basin and for the return period 475 yr (PGA). Left: smoothing method; right: zoning.

the hazard estimation. The distance disaggregations (not displayed) show expected trends with most of the contributions narrowing from 70 km at 475 yr return period to only 30 km around the site at  $10^4$  yr. Notice that the exact value of the contributing distances depends on the attenuation law used and the associated truncation.

Considering a return period of 475 yr and the frequency 2Hz (Fig. 13), the peak of 1-D contributions in magnitudes for the zoning method shifts to higher magnitudes (5.2–5.6) compared to the equivalent PGA scenarios, as intuitively expected. In the smoothing case, the 2-D disaggregations show that the  $M = 4.9$  event in the immediate vicinity of the site is still the predominant event at 2Hz.

### 4.3 Generalization: scenarios for 15 sites

#### 4.3.1 Results

The seismic scenarios are determined for 15 sites in France (locations in Fig. 1). Fig. 14 compares the evolution of the scenario magnitude with the return periods. In the zoning approach, scenario magnitudes systematically increase with increasing return periods from  $M4.5$  to  $M6.4$  (only one horizontal segment indicating that the maximum magnitude of the source zone is already reached at  $10^4$  yr). For many sites the scenario magnitude at 475 yr return period is  $M4.5$ , the minimum magnitude used in the computation. At  $10^5$  yr return period, the magnitudes range between  $M5.6$  and  $M6.4$ . In the smoothing approach, on the other hand, the scenario magnitude is often independent of the return period considered (vertical

segment in Fig. 14). In these cases, the maximum historical magnitude contributing in the neighbourhood of the site is the controlling magnitude at all return periods higher or equal to 475 yr. The scenario magnitude is very site dependent: at 475 and  $10^4$  yr return period, magnitudes range from  $M4.5$  to  $M5.7$ ; whereas at  $10^5$  yr they range between  $M5.2$  and  $M5.9$ .

#### 4.3.2 Discussion

The zoning and epicentre-smoothing approach can yield similar hazard estimates; however, by disaggregating the hazard estimates we show that the contributing magnitudes differ significantly. Disaggregation results are directly related to the seismicity models used and can lead to very different scenarios depending on the site being studied. Moreover, the contributions in magnitudes are directly related to the choice of the minimum magnitude for the low return periods, the choice of the maximum magnitude (the zoning method), or the maximum magnitude available in the seismic catalogue (smoothing method). Considering both methods equally valid, the scenarios deduced are also equally valid. In moderate seismicity regions where active faults are poorly known and where only large seismic source zones can be defined, whatever the seismicity model used, the controlling scenarios deduced from disaggregation results must be handled with great caution. Based on these results, we believe that due to the diffuse distribution of magnitude and distance contributions no single disaggregated seismic scenario can be representative of the hazard at the site.

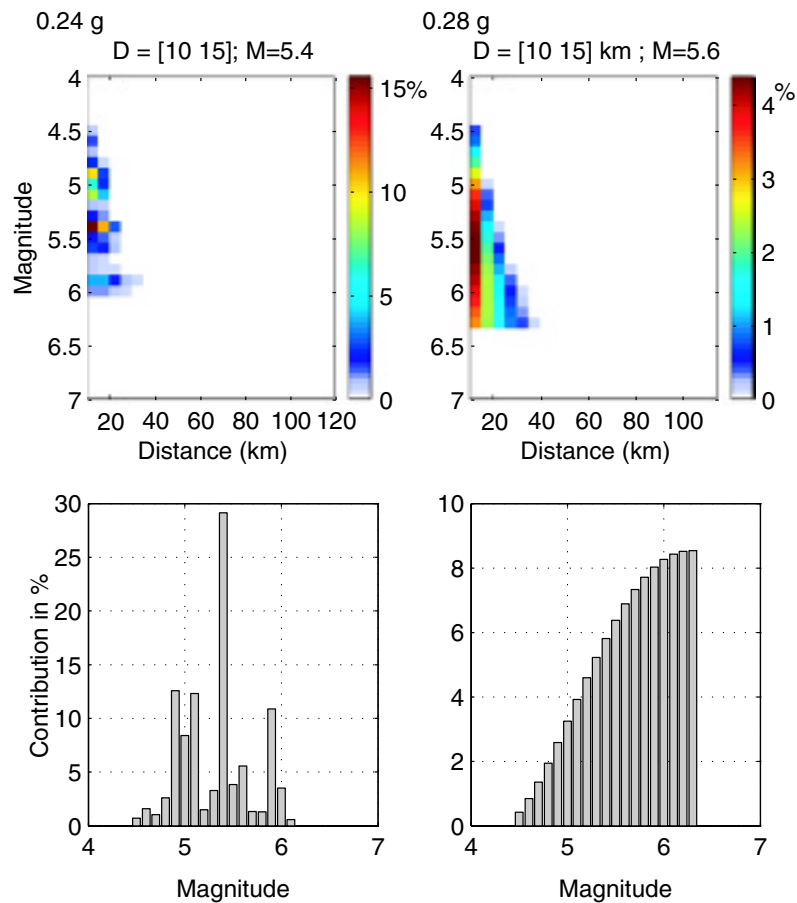


**Figure 12.** 2-D and 1-D disaggregations at the site with longitude  $7.5^\circ$  and latitude  $48.5^\circ$  located in the Rhine Basin and for the return period  $10^4$  yr (PGA). Left: smoothing method; right: zoning.

## 5 CONCLUSIONS

The aim of this study is to compare the zoning method (initially proposed by Cornell 1968) to the more recent smoothing method proposed by Woo (1996), that does not rely on source zones and recurrence curves but on maps of smoothed past epicentres locations assumed to reproduce fractal distribution of earthquakes. Both methods are compared through acceleration levels, disaggregation studies and controlling seismic scenarios. Because of such different input seismicity models, we did not anticipate the similarity of hazard levels using these two methods. Hazard levels are comparable in source zones with moderate seismic rate, whereas the epicentre-smoothing method leads to significantly lower hazard estimates where the zoning method defines narrow zones characterized by a high seismic rate. Furthermore, we show that in very low seismicity regions, the epicentre-smoothing method yields hazard estimates that are similar to the zoning method when adding a background seismicity level. The smoothing method proposed by Woo may therefore be used as a lower bound estimator for seismic hazard and in particular in very low seismicity regions where parameters required by the modelling of the frequency–magnitude distribution are very difficult to obtain.

The disaggregation studies show in detail on which sets of seismic scenarios the probabilistic estimates are based. This step is fundamental to understand the implications of the use of one model of seismicity or another. The scenarios deduced from disaggregation studies based on the smoothing and zoning approaches are similar

in distance but differ significantly in magnitude, even at locations where both methods yield identical hazard estimates. Identifying controlling earthquakes through a probabilistic approach remains thus a particularly difficult task in zones of diffuse seismicity where the most appropriate seismicity model is still a matter of debate in the scientific community. Identifying the seismic motions to be taken into account for defining the input for structural engineers will thus remain a complex task. Combining these two simple but rather different approaches, together with classical deterministic methods may, however, help the end-user community to choose from a range of reasonably possible scenarios.

## ACKNOWLEDGMENTS

Remarks and suggestions by two anonymous reviewers greatly helped improving the quality of this manuscript. We are grateful towards the Laboratoire de Détection et de Géophysique in Bruyère-le-Châtel (CEA/LDG) to have provided us the instrumental catalogue.

## REFERENCES

- Autran, A. et al., 1998. Probabilistic seismic hazard assessment in France. Part One: seismotectonic zonation, *Proceedings of the 11th ECEE, 6–11 September*, Paris, France.

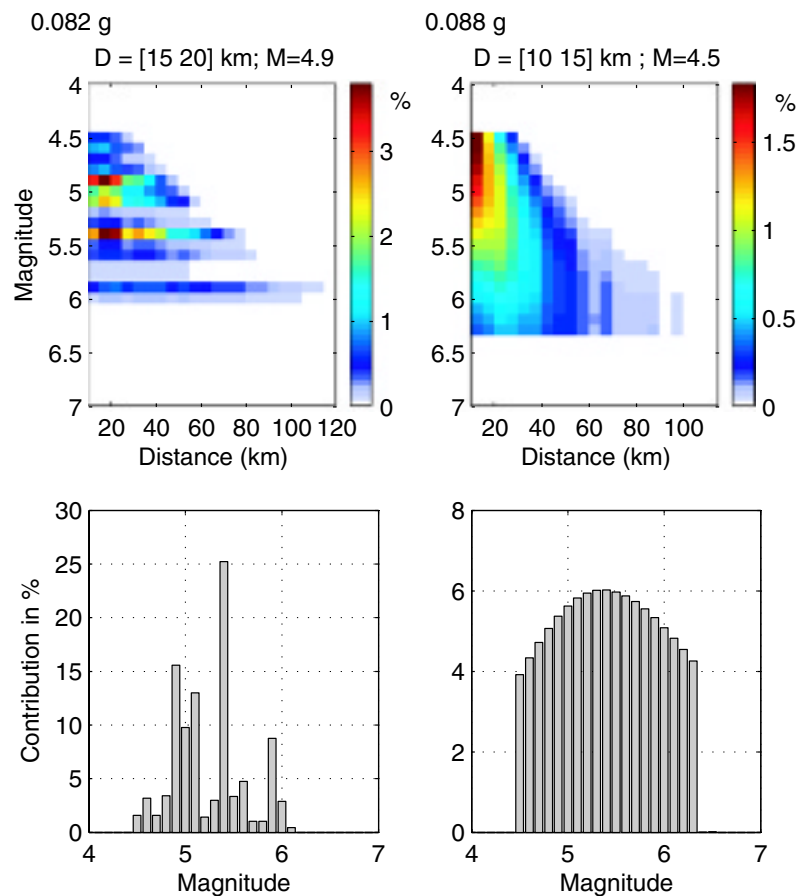


Figure 13. Same legend as Fig. 11, computations performed at 2 Hz. Left: smoothing method; right: zoning.

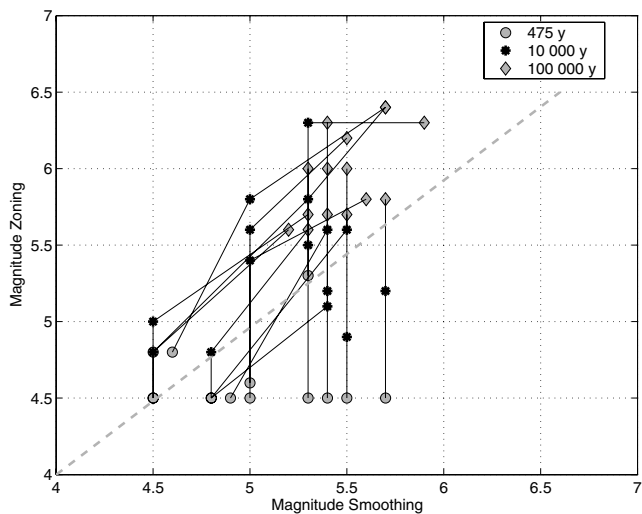


Figure 14. Magnitudes of seismic scenarios for the 15 sites shown in Fig. 1, smoothing estimate versus zoning estimate, for three return periods (segments show the evolution of the scenario magnitude for each site as a function of the return period, higher magnitude corresponds to longer return period).

Baroux, E., Pino, N.A., Valensise, G., Scotti, O. & Cushing, M.E., 2003. Source parameters of the 11 June 1909, Lambesc (Provence, south-eastern France) earthquake: a reappraisal based on macroseismic, seismological, and geodetic observations, *J. geophys. Res.*, **108**(B9), 2454, doi:10.1029/2002JB002348.

- Bazzurro, P. & Cornell, C.A., 1999. Disaggregation of seismic hazard, *Bull. seism. Soc. Am.*, **89**, 501–520.
- Beauval, C., 2003. Analyse des incertitudes dans une estimation probabiliste de l'aléa sismique, exemple de la France, *PhD Thesis*, University Joseph Fourier, France, p. 166.
- Beauval, C. & Scotti, O., 2003. Mapping  $b$ -values in France using two different magnitude ranges: possible non power-law behavior, *Geophys. Res. Lett.*, **30**, 17, 1892, doi:10.1029/2003GL017576.
- Beauval, C. & Scotti, O., 2004. Quantifying Sensitivities of PSHA for France to earthquake catalogue uncertainties, truncation of ground-motion variability, and magnitude limits, *Bull. seism. Soc. Am.*, **94**, 1579–1594.
- Bender, B.K. & Perkins, D.M., 1993. Treatment of parameter uncertainty and variability for a single seismic hazard map, *Earthquake Spectra* **9**, 2, 165–194.
- Berge-Thierry, C., Cotton, F., Scotti, O., Griot-Pommer, D. & Fukushima Y., 2003. New empirical response spectral attenuation laws for moderate European earthquakes, *Journal of Earthquake Engineering*, **7**, 193–222.
- Cao, T., Petersen, M.D. & Reichle, M.S., 1996. Seismic hazard estimate from background seismicity in Southern California, *Bull. seism. Soc. Am.*, **86**, 5, 1372–1381.
- Chapman, M.C., 1995. A probabilistic approach to ground-motion selection for engineering design, *Bull. seism. Soc. Am.*, **85**, 937–942.
- Choi, I., Choun, Y.S. & Seo, J.M., 2003. Scenario earthquakes for Korean Nuclear Power Plant Site considering active faults, XVII International Conference on Structural Mechanics in reactor technology, Prague, Czech Republic, August 17–22.
- Cornell, C.A., 1968. Engineering seismic risk analysis, *Bull. seism. Soc. Am.*, **58**, 1583–1606.
- Dominique, P. *et al.*, 1998. Part two: probabilistic approach, Seismic hazard map on the national territory (France), *Proceedings of the 11th ECEE*, 6–11 September, Paris, France.

- Frankel, A., 1995. Mapping seismic hazard in the Central and Eastern United States, *Seismological Research Letter* **66**, 4, 8–21.
- Gutenberg, B. & Richter, C.F., 1944. Frequency of earthquakes in California, *Bull. seism. Soc. Am.*, **34**, 185–188.
- Halchuck, S. & Adams, J., 2004. Deaggregation of seismic hazard for selected Canadian cities, XIII World Conference on Earthquake Engineering, Vancouver, Canada, August 1–6, 2470.
- Kagan, Y.Y. & Jackson, D.D., 1994. Long-term probabilistic forecasting of earthquakes, *J. geophys. Res.*, **99**(B7), 13 685–13 700.
- Kagan, Y.Y. & Jackson, D.D., 2000. Probabilistic forecasting of earthquakes, *Geophys. J. Int.*, **143**, 438–453.
- Kramer, S.L., 1996. Geotechnical Earthquake Engineering. Civil Engineering and Engineering Mechanics, Prentice Hall, Upper Saddle River, New Jersey 07458.
- Levret, A., Backe, J.C. & Cushing, M., 1994. Atlas of macroseismic maps for French earthquakes with their principal characteristics, *Natural Hazards*, **10**, 19–46.
- Marin, S., Avouac, J.Ph., Nicolas, M. & Schlupp, A., 2004. A probabilistic approach to seismic hazard in metropolitan France, *Bull. seism. Soc. Am.*, **94**, 2137–2163.
- Martin, Ch., Combes, Ph., Secanell, R., Lignon, G., Carbon, D., Fioravanti, A. & Grellet, B., 2002a. Révision du zonage sismique de la France. Etude probabiliste, Rapport GEOTER GTR/MATE/0701-150.
- Martin, Ch., Secanell, R., Combes, Ph., Lignon, G., 2002b. Preliminary probabilistic seismic hazard assessment of France, Proceedings of the 12th ECEE, Paper reference 870, September, London, England.
- McGuire, R.K., 1976. Fortran computer program for seismic risk analysis, *US Geological Survey open-File Report* 76–67.
- Molina, S., Lindholm, C.D. & Bungum, H., 2001. Probabilistic seismic hazard analysis: zoning free versus zoning methodology, *Bollettino di Geofisica*, selected papers from the 27th ESC, Lisbon, 2000, **42**, 19–39.
- Nicolas, M., Bethoux, N. & Madeddu, B., 1998. Instrumental seismicity of the Western Alps: a revised catalogue, *Pure appl. Geophys.*, **152**, 707–731.
- Vere-Jones D., 1992. Statistical methods for the description of and display of earthquake catalogues, in *Statistics in the Environmental and Earth Sciences*, pp. 220–244, eds. Walden A.T. and Guttorp P., London.
- Weichert, D.H., 1980. Estimation of the earthquake recurrence parameters for unequal observation periods for different magnitudes, *Bull. seism. Soc. Am.*, **70**, 4, 1337–1346.
- Woo, G., 1996. Kernel estimation method for seismic hazard area source modeling, *Bull. seism. Soc. Am.*, **86**, 2, 353–362.